Langmuir
Article
pubs.acs.org/Langmuir

Tuning Curvature in Flow Lithography: A New Class of Concave/Convex Particles

Priyadarshi Panda, Kai P. Yuet, T. Alan Hatton, and Patrick S. Doyle*

Department of Chemical Engineering, Massachusetts Institute of Technology, 77 Massachusetts Avenue, Cambridge, Massachusetts 02139

Received December 23, 2008. Revised Manuscript Received February 3, 2009

Polymeric particles of complex shapes and chemistry have been used for a wide variety of applications in the materials and bioengineering fields. An interesting means of introducing complexity is through curvature. In this work, stop-flow lithography is used to generate concave/convex particles at high throughputs of 3×10^4 particles/h. These particles have finely tuned curvature in the plane orthogonal to the plane of projection of light. The shape in the plane of projection of light is determined by the mask shape. The chemical programmability of this technique is further demonstrated by creating multifunctional particles, i.e., patchy and capped particles. The directed assembly of these particles can find potential application in a variety of fields like biology, photonics, and liquid crystals.

Introduction

Polymeric particles of complex architecture are widely used for applications such as photonic materials,[1] MEMS,[2] biomaterials,[3] and self-assembly.[4] Introducing complexity in particle design is important since particle shape can significantly influence particle function.[5] An important facet of shape complexity is the introduction of curvature. It has been shown by molecular simulations that the curvature of particles can be tuned to regulate assembly as demonstrated by viral assembly.[6] Experimental evidence has also been provided for the preferential standing positions of concavo-convex particles with clear analogy to brachiopod or pelecypod shell orientation in moderately turbulent water.[7] Curvature, both convex and concave, can thus be used to tune assembly of particles,[6,7] leading to breaking of point symmetries (lower symmetries than spherical particles) for photonic materials,[8] generation of scaffolds of desired curvature for directing cell internal organization,[9] and improved osteoblast performance for significant bone tissue formation.[10] Particles with finely tuned curvature can also be used for facilitating or hindering phagocytosis,[11] studying scattering functions of aerosols,[12] and acquiring experimental evidence on scattering dependence on concavity for polyhedral ice crystals for atmospheric science.[13] Furthermore, curved nonspherical particles have applications in cosmetics[14] and can be used for fundamental studies in microfluidics[15] and generation of diverse crystal structures.[16] The synthesis of nonspherical particles and the role of shape anisotropy in assembly have been demonstrated by Stroock et al.[17] Further, work has also been done to demonstrate the synthesis and assembly of structured colloidal particles with control over size, shape, and structure and their application in photonics.[18−20] Lastly, nonspherical particles may also open new applications in advanced materials due to their unique scattering properties.[21]

Current approaches to particle synthesis are either nonmicrofluidic batch[22−28] or continuous[28] processes or microfluidic schemes which are based on two-phase flow[29−34] or

*Corresponding author. E-mail: pdoyle@mit.edu.

(1) Lu, Y.; Yin, Y.; Xia, Y. *Adv. Mater.* **2001**, *13*, 415.
(2) Beebe, D. J.; Moore, J. S.; Bauer, J. M.; Yu, Q.; Liu, R. H.; Devadoss, C.; Jo, B.-H. *Nature (London)* **2000**, *404*, 588.
(3) Langer, R.; Tirell, D. A. *Nature (London)* **2004**, *428*, 487.
(4) Glotzer, S. C. *Science* **2004**, *306*, 419.
(5) Champion, J. A.; Katare, Y. K.; Mitragotri, S. *Proc. Natl. Acad. Sci. U. S.A.* **2007**, *104*, 11901.
(6) Chen, T.; Zhang, Z.; Glotzer, S. C. *Proc. Natl. Acad. Sci. U.S.A.* **2007**, *104*, 717.
(7) Middleton, G. V. *J. Sediment. Petrol.* **1967**, *327*, 229.
(8) Xia, Y.; Gates, B.; Yin, Y.; Lu, Y. *Adv. Mater.* **2000**, *12*, 693.
(9) Théry, M.; Racine, V.; Piel, M.; Pépin, A.; Dimitrov, A.; Chen, Y.; Sibarita, J.-B.; Bornens, M. *Proc. Natl. Acad. Sci. U.S.A.* **2006**, *103*, 19771.
(10) Graziano, A.; d'Aquino, R.; Gabriella, M.; Angelis, C.-De; Laino, G.; Piattelli, A.; Pacifici, M.; De Rosa, A.; Papaccio, G. *PLoS ONE* **2007**, *6*, e496.
(11) Champion, J. A.; Mitragotri, S. *Proc. Natl. Acad. Sci. U.S.A.* **2006**, *103*, 4930.
(12) Koepke, P.; Hess, M. *Appl. Opt.* **1988**, *27*, 2422.
(13) Macke, A. *Appl. Opt.* **1993**, *32*, 2780.
(14) USA Patent 20070154500.
(15) Mason, T. G.; Ganeshan, K.; vanZanten, J. H.; Wirtz, D.; Kuo, S. C. *Phys. Rev. Lett.* **1997**, *79*, 3282.
(16) van der Kooij, F. M.; Kassapidou, K.; Lekkerkerker, H. N. W. *Nature (London)* **2000**, *406*, 868.
(17) Badaire, S.; Cottin-Bizonne, C.; Woody, J. W.; Yang, A.; Stroock, A. D. *J. Am. Chem. Soc.* **2007**, *129*, 40.
(18) Yang, S.-M.; Kim, S.-H.; Lim, J.-M.; Yi, G.-R. *J. Mater. Chem.* **2008**, *18*, 2177.
(19) Kim, S.-H.; Jeon, S.-J.; Yang, S.-M. *J. Am. Chem. Soc.* **2008**, *130*, 6040.
(20) Kim, S.-H.; Jeon, S.-J.; Yi, G.-R.; Heo, C.-J.; Choi, J. H.; Yang, S.-M. *Adv. Mater.* **2008**, *20*, 1649.
(21) Manoharan, V. N.; Pine, D. J. *Mater. Res. Soc. Bull.* **2004**, *29*, 91.
(22) Brown, A. B. D.; Smith, C. G.; Rennie, A. R. *Phys. Rev. E* **2000**, *62*, 951.
(23) Love, J. C.; Wolfe, D. B.; Jacobs, H. O.; Whitesides, G. M. *Langmuir* **2001**, *17*, 6005.
(24) Revzin, A.; Russel, R. J.; Yadavalli, V. K.; Koh, W.-G.; Deister, C.; Hile, D. D.; Mellott, M. B.; Pishko, M. V. *Langmuir* **2001**, *17*, 5440.
(25) Jiang, P.; Bertone, J. F.; Colvin, V. L. *Science* **2001**, *291*, 453.
(26) Sugiura, S.; Nakajima, M.; Tong, J.; Nabetani, H.; Seki, M. *J. Colloid Interface Sci.* **2000**, *227*, 95.
(27) Hernandez, C. J.; Mason, T. G. *J. Phys. Chem. C* **2007**, *111*, 4477.
(28) Rolland, J. P.; Maynor, B. W.; Euliss, L. E.; Exner, A. E.; Denison, G. M.; DeSimone, J. M. *J. Am. Chem. Soc.* **2005**, *127*, 10096.
(29) Nisisako, T.; Torii, T.; Higuchi, T. *Chem. Eng. J.* **2004**, *101*, 23.
(30) Dendukuri, D.; Tsoi, K.; Hatton, T. A.; Doyle, P. S. *Langmuir* **2005**, *21*, 2113.
(31) Xu, S.; Nie, Z.; Seo, M.; Lewis, P.; Kumacheva, E.; Stone, H. A.; Garstecki, P.; Weibel, D. B.; Gitlin, I.; Whitesides, G. M. *Angew. Chem., Int. Ed.* **2005**, *44*, 724.
(32) Jeong, W.; Kim, J.; Kim, S.; Lee, S.; Mensing, G.; Beebe, D. J. *Lab Chip* **2004**, *4*, 576.
(33) Subramaniam, A. B.; Abkarian, M.; Stone, H. A. *Nat. Mater.* **2005**, *4*, 553.
(34) Nisisako, T.; Torii, T. *Adv. Mater.* **2007**, *19*, 1489.

continuous-flow lithography (CFL)[35] and its variant stop-flow lithography (SFL).[36] SFL is a versatile technique which has been used to generate cell-encapsulated hydrogels,[37] ceramic microcomponents,[38] and barcoded particles for biomolecular analysis.[39] Another noteworthy microfluidic-based technique for generating complex microparticles forms polystyrene microbeads into higher order assemblies via microfluidic arrangement and thermal fusion.[40]

The limitations of batch processes like traditional photolithography include the low throughput and the inability to pattern high-resolution features using low-viscosity oligomers. Flow-through microfluidic schemes based on two-phase flow can be used to generate spherical particles or modifications thereof, e.g., disks due to surface tension restrictions.[30,31] These structures are therefore inherently convex. Convex particles have also been generated recently by several groups using nonmicrofluidic schemes.[5,41] Traditional photolithography and CFL/SFL can be used together to create concave architecture using suitably designed masks; however, the structures formed are essentially 2D extruded structures, having straight walls in the direction orthogonal to the direction of projection of light. Techniques for generating truly 3D nonconvex (concave) particles with precise control over particle curvature are therefore needed. The Thomas group recently introduced concave curvature in polymeric particles using holographic interference lithography (HIL) which to the best of our knowledge is the only work of its kind. However, at present, their technique is only capable of creating single chemistry particles.[42]

The purpose of this article is to tune the curvature (concavity/convexity) in flow lithography and generate a new class of microparticles. The introduction of curvature in the direction orthogonal to the incident light in conjunction with curvilinear photomask geometry gives rise to a new class of microparticles. The importance of introducing curvature in particles can be explained by a simple example related to assembly of these particles: a flat surface generated via photolithography using a mask with a rectangular feature has flat sides with line or point valence of zero. The introduction of concavity of radius R_1 in the plane of UV light on one side or two opposite sides of the rectangular mask introduces a line valence of 2 and 4, respectively. The introduction of concavity with a radius R_2 in the plane orthogonal to the direction of projection of light in addition to R_1 in the plane of light leads to a point valence of 4 and line valence of 2 or a point valence of 8 and line valence of 0 depending on curvature being introduced on a single side or both sides in the plane orthogonal to projection of light.[42] These three different classes of particles would assemble differently,[42] giving entirely unique photonic structures, liquid crystals, or scaffolds.

A new class of particles which we call "dual curvature in a plane particle" can be synthesized by this technique. These are particles which have two radii of curvature (R_1, R_2) cut out from a plane. The addition of this second radius of curvature can be used to modulate the strength of specific interactions. It has been shown that the adhesive strength of nonspherical particles mediated by specific interactions is greater than spherical particles under a linear shear flow.[43] The presence of curvature in two orthogonal axes R_1 and R_2 ($R_1 > R_2$) for instance can also be used to selectively isolate particles of a certain size range ($R_2 <$ particle size $< R_1$) from a polydisperse group of particles. This kind of tuning wherein a maximum and a minimum (curvatures in orthogonal axes) can be controlled independently has not been demonstrated in hitherto known particles.

The chemical programmability of this technique is demonstrated by synthesizing Janus, patched, and capped polymeric particles. The presence of patches on particles is analogous to valence in atoms and can be used to tune the relative strength and direction of interactions between particles, leading to tuning of the final assembled structures.[44] Capped particles (particles having a cap/brush of a different chemistry) are another interesting addition to the existing class of curved particles that we introduce in this work. Capped particles have potential applications for directed assembly and selective adhesion for example. The ability to pattern curved surfaces can be used to select and isolate molecules of different chemistries from a mixture by putting markers on the patterning or capping fluid.

Experimental Section

Materials. All the particles synthesized in this work are either made from tri(methylolpropane) triacrylate (TMPTA, Polysciences) or poly(ethylene glycol) (700) diacrylate (PEG-DA, Sigma Aldrich). The capping fluid (C) contained poly(ethylene glycol) (375) acrylate (PEG-acrylate, Sigma Aldrich). For the experiments involving fluorescence, a solution containing 0.01 wt % of methacryloxyethylthiocarbamoyl rhodamine B (Polysciences, M-acryl-rhodamine B) in PEG-DA, TMPTA, or PEG-acrylate was used. The compositions of the polymerization fluid (P), tuning fluid (T), and capping fluid (C) are given in Table 1.

Microfluidic Devices and Photopolymerization Setup. Photomasks were designed using AutoCAD 2005 and sent to CAD Art Services (Poway, CA) where they were printed using a high-resolution printer. The appropriate mask was then inserted into the field stop of the microscope and UV light flashed through it from a 100 W HBO mercury lamp once the flow was stopped. A filter set that allowed wide UV excitation (11000v2: UV Chroma) was used to filter out light of undesired wavelengths. The devices used in this work were fabricated by pouring polydimethylsiloxane (PDMS, Sylgard 184, Dow Corning) on a silicon wafer containing positive-relief channels patterned in SU-8 photoresist (Microchem). The devices were rectangular channels of two different heights (30 or 60 μm) and had a width of 200 μm for the experiments wherein two streams were coflown, single height (60 μm) and a width of 300 μm for the experiments wherein three streams were coflown, and a single height (50 μm) and a width of 300 μm for the experiments wherein four streams were coflown. The PDMS devices were sealed to glass slides spin-coated with PDMS to ensure that all four walls of the channel were PDMS. The devices were mounted on an inverted microscope (Axiovert 200, Zeiss), and the formation of microparticles was visualized using a CCD camera (KPM1A, Hitachi). Fluorescent and bright-field images of particles were obtained using a digital camera (Nikon, D-200).

(35) Dendukuri, D.; Pregibon, D. C.; Collins, J.; Hatton, T. A.; Doyle, P. S. *Nat. Mater.* **2006**, *5*, 365.
(36) Dendukuri, D.; Gu, S. S.; Pregibon, D. C.; Hatton, T. A.; Doyle, P. S. *Lab Chip* **2007**, *7*, 818.
(37) Panda, P.; Ali, S.; Lo, E.; Chung, B. G.; Hatton, T. A.; Khademhosseini, A.; Doyle, P. S. *Lab Chip* **2008**, *8*, 1056.
(38) Shepherd, R.; Panda, P.; Bao, Z.; Sandhage, K. H.; Hatton, T. A.; Lewis, J.; Doyle, P. S. *Adv. Mater.* **2008**, *20*, 4734.
(39) Pregibon, D. C.; Toner, M.; Doyle, P. S. *Science* **2007**, *315*, 1393.
(40) Sung, K. E.; Vanapalli, S. A.; Mukhija, D.; McKay, H. A.; Millunchick, J. M.; Burns, M. A.; Solomon, M. J. *J. Am. Chem. Soc.* **2007**, *130*, 1335.
(41) Jeon, S.; Malyarchuk, V.; Rogers, J. A.; Wiederrecht, G. P. *Opt. Express* **2006**, *14*, 2300.
(42) Jang, J.-H.; Ullal, C. K.; Kooi, S. E.; Koh, C. Y.; Thomas, E. L. *Nano Lett.* **2007**, *7*, 647.
(43) Decuzzi, P.; Ferrari, M. *Biomaterials* **2006**, *27*, 5307.
(44) Glotzer, S. C.; Solomon, M. J. *Nat. Mater.* **2007**, *6*, 557.

Table 1. List of Polymerization (P) and Tuning (T) Fluids Used in This Article

fluid code	composition
P1	TMPTA (95%) + Darocur 1173 (5%)
P2	PEG-DA (55%) + water (40%) + Darocur 1173 (5%)
P3	PEG-DA (55%) + water (40%) + Darocur 1173 (5%) + M-acryl-rhodamine B (0.01%)
P4	TMPTA (95%) + Darocur 1173 (5%) + M-acryl-rhodamine B (0.01%)
T1	PEG-DA (68%) + water (32%)
T2	glycerol (85%) + water (15%)
T3	silicone oil
C1	PEG-acrylate (65%) + water (35%) + M-acryl-rhodamine B (0.01%)

Surface Tension Measurements. Surface tension measurements were carried out using the pendant drop method and a DSA 10 tensiometer (Kruss). Contact angle measurements were carried out using the sessile drop method and the same tensiometer. Advancing contact angle was measured for a drop of liquid on a clean PDMS slab.

Particle Recovery and Characterization. The particles were collected in the reservoir of the microchannel and washed three times using ethanol. For fluorescent experiments the particles in the reservoir were washed with ethanol 10 times, pipetting ethanol in and out, and thus mixing the contents of the reservoir, in each wash. Images of the polymeric particles were saved at different points in the reservoir, and 35 particles from these images were used for calculating the coefficient of variation (COV). These particles were then pipetted out using ethanol solution and collected in an Eppendorf tube. The Eppendorf tube was centrifuged to allow the particles to settle down, the supernatant was removed, new ethanol was added, and the contents were vortex mixed. This procedure of centrifugation, removing supernatant (ethanol), adding new ethanol, and vortex mixing the contents, was repeated three times to obtain a collection of the particles suspended in clean (oligomer-free) ethanol.

Results and Discussion

A schematic diagram of the setup is shown in Figure 1A. A photocurable solution which we call the polymerization fluid (P) and a nonphotocurable solution, named tuning fluid (T), are coflowed and then stopped. Curvature develops at the interface of the two fluids which depends on the surface energies of the P, T, and the walls of the microchannel. The quiescent fluids are exposed to a flash of UV light through a photomask. The region of the P exposed to the UV light is polymerized while T is an inert (nonpolymerizing) fluid. This leads to the generation of a polymeric particle having a shape in the plane of projection of light determined by the mask and a curvature in the plane orthogonal to the plane of light determined by three parameters: (a) the surface energies of the P and T, (b) the surface energies of the bottom and top wall of the microchannel, and (c) the height of the channel. The particles are then flushed out of the channel and collected in a reservoir at the end of the channel.

The curvature is illustrated in Figure 1B. The radius of curvature (R) and the maximum deformation (D_{max}) for a channel of height H are given by

$$R = \frac{H}{2\cos\beta} \tag{1}$$

$$D_{max} = \frac{H(1-\sin\beta)}{2\cos\beta} = R(1-\sin\beta) \tag{2}$$

A simple force balance can be used to evaluate $\cos\beta$ using the equation

$$\gamma_{PT}\cos\beta = \gamma_{TS} - \gamma_{PS} \tag{3}$$

where γ_{PT} is the interfacial tension between the T and P and γ_{TS} and γ_{PS} are the solid−liquid interfacial tensions between PDMS (S) and the T and P, respectively. The right-hand side of eq 3 can be evaluated by conventionally measurable properties like the contact angle of the T and P on a PDMS surface surrounded by air and the surface tensions of pure T and P:

$$\gamma_{TS} = \gamma_{AS} - \gamma_{TA}\cos\theta_T \tag{4}$$

$$\gamma_{PS} = \gamma_{AS} - \gamma_{PA}\cos\theta_P \tag{5}$$

where γ_{AS} is the surface tension of the PDMS surface and γ_{TA} and γ_{PA} are the surface tensions of T and P, respectively. θ_T and θ_P are the contact angles of the T and P, respectively. Subtracting eq 5 from eq 4, we attain

$$\gamma_{TS} - \gamma_{PS} = \gamma_{PA}\cos\theta_P - \gamma_{TA}\cos\theta_T \tag{6}$$

Using eqs 1, 3, and 6, we get

$$R = \frac{H\gamma_{PT}}{2(\gamma_{PA}\cos\theta_P - \gamma_{TA}\cos\theta_T)} \tag{7}$$

$$D_{max} = R(1-\sin\beta) = \frac{H\gamma_{PT}(1-\sin\beta)}{2(\gamma_{PA}\cos\theta_P - \gamma_{TA}\cos\theta_T)} \tag{8}$$

We investigated the predictability of the curvature (R and D_{max}) by varying two of the three tuning parameters, i.e., the tuning fluid and the height of the channel. The values for the different parameters used in eqs 7 and 8 for the two Ts used are reported in Table S1 (see Supporting Information) and the comparison between the experimentally measured (using 35 particles) and theoretically estimated R and D_{max} are reported in Table S2 (see Supporting Information). Figure 1C shows an example of particle R and D_{max} measured experimentally. It can be seen from Table S2 that the theoretically predicted curvatures are in excellent agreement with experimentally obtained values with the maximum deviation in R and D_{max} being 3.7% and 8.0%, respectively, for the three cases (two different Ts and heights) studied.

We quantified the monodispersity of the particles obtained with respect to the curvature in the plane orthogonal to the direction of projection of light, using the batch of particles obtained for Figure 1C. The COV in the radial direction was found to be 4% using a sample of 35 particles. We have previously ascertained that the COV for our particles along the plane of projection of light is less than 2.5%.[45] We can therefore conclude that the particles generated by this technique are monodisperse since the COV is $< 5\%$.[46] We were able to obtain a throughput of $\sim 3 \times 10^4$ particles/h for these particles, using a mask having seven rectangular features in a

(45) Dendukuri, D.; Hatton, T. A.; Doyle, P. S. *Langmuir* **2007**, *23* 4669.

(46) Jillavenkatesa, A.; Dapkunas, S. J.; Lum, L.-S. H. Particle Size Characterization; Technical Report 960; National Institute of Standards and Technology (NIST); U.S. Government Printing Office: Washington, DC, **2001**.

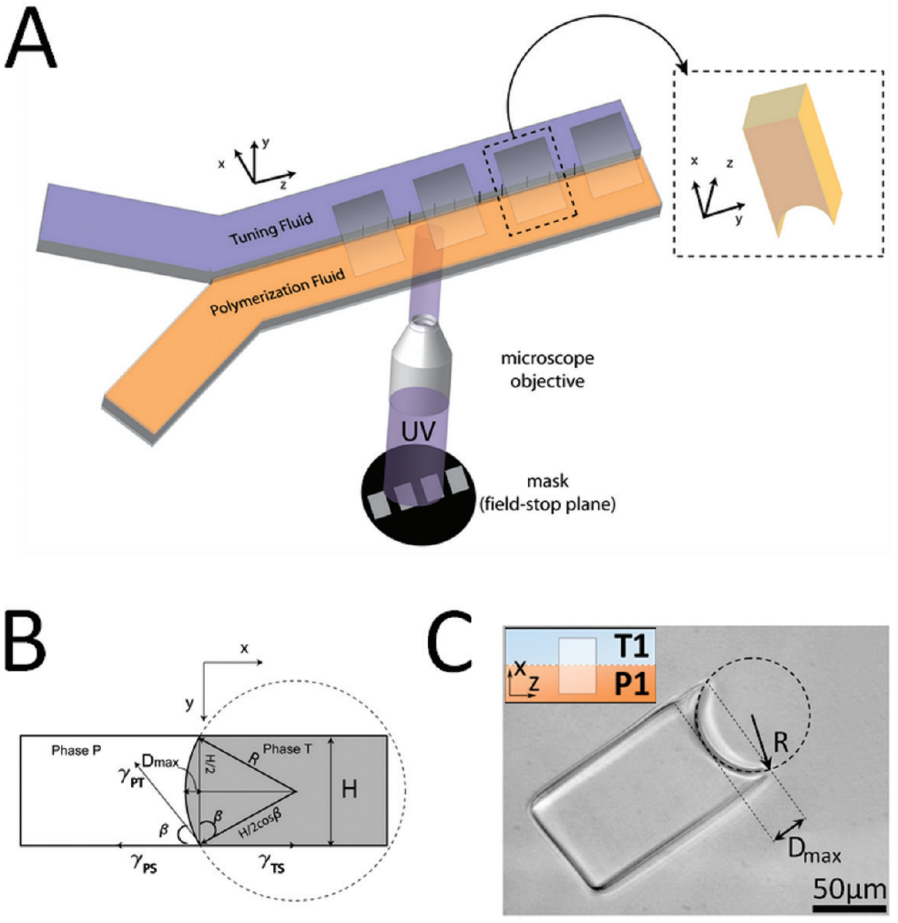

Figure 1. (A) Schematic illustration of concave particle synthesis using stop flow lithography (SFL) system. Photocurable solution (polymerization fluid) and tuning fluid are coflowed and then stopped. Depending on the relative surface energies, curvature develops at the interface between the immiscible fluids (inset). Ultraviolet light is then projected through a mask, solidifying polymeric particles having the shape on the $x-z$ plane determined by the mask and the shape in the $x-y$ plane determined by the equilibrium curvature. The section of the tuning fluid exposed to UV light does not get polymerized. (B) Schematic showing the cross section of the microfluidic device and the radius of curvature (R) and maximum deformation (D_{max}) of the particles on the $x-y$ plane. (C) Differential interference contrast (DIC) image of the cross-sectional view of the curvature of a TMPTA particle. The particle was synthesized in a 60 μm tall channel.

row, using typical stop, polymerization, and flow times of 100, 60, and 600 ms, respectively.

Choosing the Tuning and Polymerization Fluids. Having established the physical parameters for the tuning of curvature, we ascertained the pair of Ts and Ps to be used for synthesizing curved polymeric particles to demonstrate both the materials flexibility and the tuning of curvature. The materials flexibility is demonstrated by making TMPTA (hydrophobic) and PEG-DA (hydrophilic) particles. When selecting a T, we ensured that it was inert and the T and P do not flip over. Flipping over is the process in which a gravity-induced pressure mismatch at the interface gradually drives the denser fluid to occupy the lower portion of the microchannel. The rate of this process depends on the interplay between the viscous forces which tend to dominate at the microscale and the gravitational forces.[47] While density mismatch favors the flipping over of the fluids, viscous forces favor coflow and dampen the propensity to flip over. In our case, since the T and P are immiscible, in addition to the viscous and gravity forces, the surface forces need to be accounted for. For channels of aspect ratio 1, interfacial force attenuates the effect of gravity.[48] A glycerol−water mixture, 85% (v/v) glycerol (ρ = 1.22 g/cm^3), was chosen as the T for generating concave TMPTA (ρ = 1.12 g/cm^3) particles. Because of the high viscosity of these solutions (~106 cP), the interface does not flip over in spite of the density mismatch. Mineral oil (ρ = 0.8 g/cm^3), corn oil (ρ = 0.9 g/cm^3), PDMS (ρ = 0.98 g/cm^3), and silicone oil (ρ = 1.05 g/cm^3) were tried as potential Ts for generating PEG-DA particles. For mineral oil, corn oil, and PDMS, the density mismatch with PEG-DA (ρ = 1.12 g/cm^3) and low viscosities led to distorted interfaces. Silicone oil was chosen as the T due to closer density to PEG-DA. A diluted PEG-DA solution (40% water) was used as the P. The increased hydrophilicity due to the dilution by water accentuated the convex curvature. The Ps and Ts used in this article are listed in Table 1.

Classification Scheme. Concave/convex particles were synthesized using different masks as shown in Figure 2. The simplest classification scheme for these particles is based on the number of faces, line valences, and point valences present in the particle in the planes orthogonal to the plane of projection of light.[42] The illustration in Figure 3 demonstrates the transition from a flat surface (Figure 3A) to a two line valence (Figure 3B) and four point valence (Figure 3C) structures by the successive addition of one and two curvatures, respectively.

(47) Yoon, S. K.; Mitchell, M.; Choban, E. R.; Kenis, P. J. A. *Lab Chip* **2005**, *5*, 1259.
(48) Yamaguchi, Y.; Honda, T.; Briones, M. P.; Yamashita, K.; Miyazaki, M.; Nakamura, H.; Maeda, H. *Chem. Eng. Technol.* **2007**, *30*, 379.

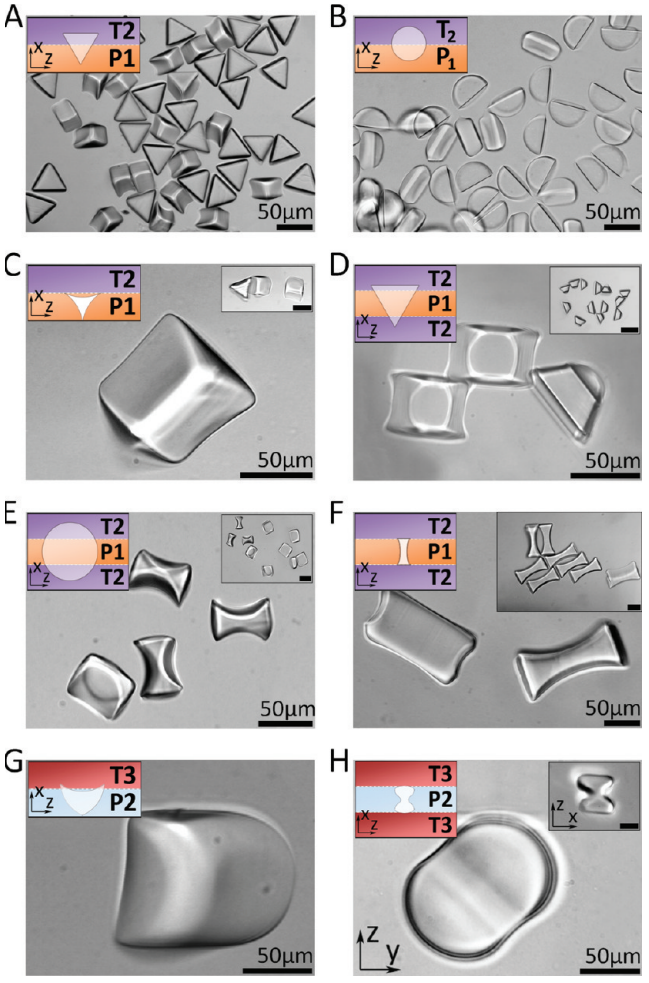

Figure 2. DIC images of curved particles of single chemistry. The particles have curvature in the direction orthogonal to the direction of projection of light. The schematic at the top left-hand corner of the images shows the mask feature and the fluids used (see Table 1). (A) Concave triangles generated in a 60 μm tall channel. (B) Concave half-disks generated in a 30 μm tall channel. (C) Particles with three concave edges in the plane of projection of light and a concave edge in the plane orthogonal to the plane of projection of light (dual curvature in a plane structure). (D, E, and F) Concavo-concave particles generated using a 60 μm tall channel and a triangular, circular, and distorted rectangle mask feature, respectively. (G) Convex particles generated using a 60 μm tall channel demonstrating the same duo curvature along a plane structure but the curvatures being concave-convex. The image shows the convex curvature imposed on the concave curvature which is visible only at the center of that edge where the radius of concavity in the plane of projection of light is greater than the convexity in the plane orthogonal to the plane of projection of light. (H) Convexo-convex particles generated in a 60 μm tall channel using a distorted rectangular mask feature having opposite edges defined by the Chebyshev polynomial of first kind and fourth order. (A−F) are TMPTA particles while (G, H) are PEG-DA particles.

Concave Particles. Figure 2A demonstrates the generation of a structure with two line valences from a triangular mask feature. Traditional photolithography would generate a structure with a line valence of zero. A circular mask feature is of considerable interest as a circle is a closed figure with zero corners. Figure 2B demonstrates the use of a circular mask feature which forms a structure with two line valences, along the edge parallel to the interface of the coflowing fluids and having concavity and convexity in orthogonal planes. Figure 2C demonstrates the generation of a structure with

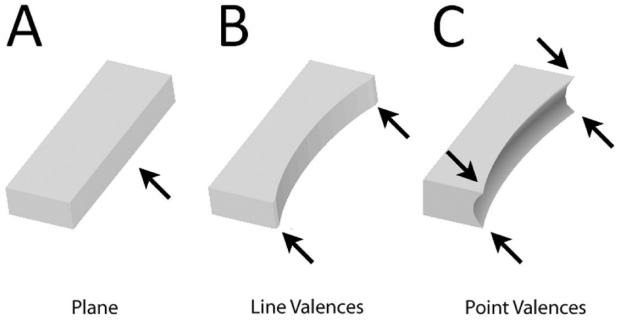

Figure 3. Illustration demonstrating the transition from a flat surface (A) to two line valence (B) and four point valence (C) structures by the successive addition of one and two curvatures, respectively.

one line valence and four point valences by using a mask feature with three curved edges, one of them, aligned parallel to the interface between the coflowing fluids. It also shows the generation of a hollow structure with two radii of curvature along orthogonal directions (dual curvature in a plane particle).

Concavo-Concave Particles. Figure 2D shows the formation of a concavo-concave structure with four line valences using a triangular mask feature. Figure 2E shows the generation of a particle with four line valences having convexo-convex and concavo-concave structures on orthogonal planes. Figure 2F demonstrates the use of a four-cornered mask feature aligned with two opposite edges parallel to the two interfaces of the P and the Ts. The particle has concavo-concave curvatures on orthogonal planes. Furthermore, because of the alignment of the straight edges along the interface, it gives rise to a particle with four line valences. The alignment of the curved edges along the interface of the P and the Ts would have given rise to a structure with eight point valences and two faces.

Convex and Convexo-Convex Particles. The materials flexibility is demonstrated by generating convex and convexo-convex PEG-DA particles as shown in parts G and H of Figure 2, respectively. The particles in Figure 2G had the concave edge aligned along the interface of the two fluids (illustration Figure 2G), and thus a polymeric particle with one line valence and four point valences was generated. This particle has a concave and convex edge along orthogonal planes cut out from a plane, i.e., demonstrates a "dual curvature in a plane particle". Figure 2G shows the convex curvature superimposed on the concave curvature, which is visible only at the center of that edge, where the radius of concavity in the plane of projection of light is greater than the convexity in the plane orthogonal to the plane of projection of light. The structures generated until this point demonstrated the use of straight lines or simple curvatures (concave or convex) along the edge of the *n*-cornered mask feature. Figure 2H shows the use of a polynomial (Chebyshev polynomial of the first kind and fourth order)[49] as two opposite edges in a distorted rectangular mask feature. The mask had two straight edges which were aligned along the two interfaces of the Ts and the P and two curved edges (defined by the Chebyshev polynomial) along the other opposite edges. The polymeric particle thus formed is a Chebyshev particle with four line valences.

(49) Weisstein, E. W. "Chebyshev Polynomial of the First Kind" can be found under http://mathworld.wolfram.com/ChebyshevPolynomialof- -the-FirstKind.html, **2008**.

Multifunctional Particles. Janus particles with convexity in the polymerization plane on the PEG-DA part and concavity in the plane orthogonal to the projection of light on the TMPTA part are shown in Figure 4A. These particles have alternate curvatures in perpendicular plains on two different chemistries. Similarly, Figure 4B demonstrates the ability to create concave and convex architecture in a plane orthogonal to the direction of projection of light in the same particle, the curvatures being on different chemistries, PEG-DA (convex)−TMPTA (concave). These particles can be synthesized using SFL (shown only for easy imaging and visualization). A triangular feature on a mask was used to generate convexo-concave particles shown in Figure 4C.

Patterned Chemistries. The chemical programmability of this technique was demonstrated by making patchy and capped particles. The essential difference between patchy and capped particles lies in the properties of the fluid used for generating the pattern. The P used for creating a patch is a cross-linkable oligomeric fluid (multifunctional, diacrylate for instance) with photoinitiator. On exposure to UV light, free radicals are generated due to the presence of the photoinitiator and the diacrylate cross-links to form a gel. The capping fluid (C), on the other hand, is a polymerizable but non-cross-linkable oligomeric fluid (monofunctional, monoacrylate for instance) with no photoinitiator. When C is exposed to UV light, free radicals are not generated in the bulk fluid due to the absence of photoinitiator. However, the coflowing P undergoes gelation on exposure to UV light. Free radicals at the P−C interface can lead to polymerization of the oligomer in C which results in a linear polymer that is attached by one end to the particle created in the P solution. The resulting structure will be a thin polymer brush on the curved face of the particle.

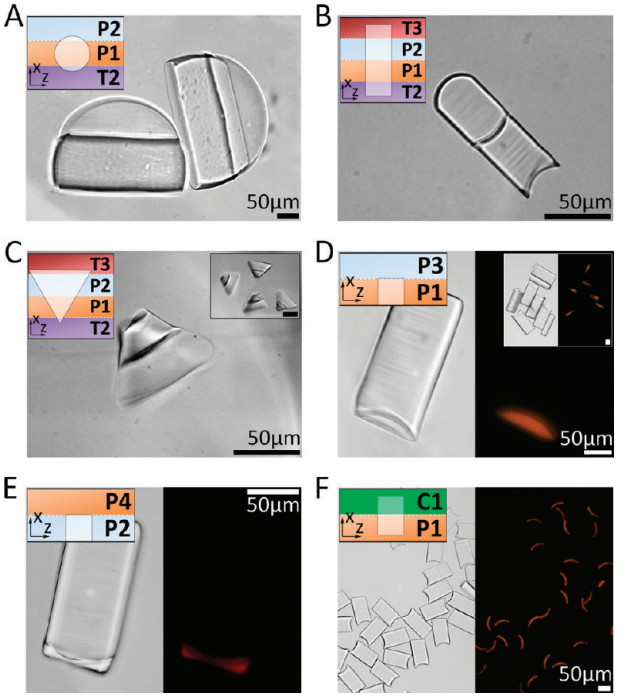

Figure 4. DIC images of curved particles containing multiple chemistries. The particles have curvature in the direction orthogonal to the direction of projection of light. The schematic at the top left-hand corner of the images shows the mask feature and the fluids used (see Table 1). (A) Concave Janus half-disks made from PEG-DA and TMPTA depicting curvature in two different chemistries in orthogonal axis. (B, C) Concavo-convex particles containing two chemistries (PEG-DA and TMPTA). (D) Bright field and fluorescence image of patchy particles having PEG-DA patch on TMPTA particles. The PEG-DA region contains rhodamine acrylate and hence glows red in the fluorescence image while the TMPTA part is not fluorescent. (E) Bright field and fluorescence image of patchy particles having TMPTA patch on PEG-DA particles. The TMPTA region contains rhodamine acrylate and hence glows red in the fluorescence image while the PEG-DA part is not fluorescent. (F) Bright field and fluorescence image of capped particles containing PEG acrylate cap on concave TMPTA particles. The PEG-acrylate caps contain rhodamine acrylate.

We generated patchy particles having PEG-DA patches on TMPTA particles and the inverse TMPTA patches on PEG-DA particles as shown in parts D and E of Figure 4, respectively. The TMPTA particles have four TMPTA faces and two opposite faces having a curved PEG-DA patch, as shown in Figure 4D, while PEG-DA particles have two opposite PEG-DA faces, two opposite PEG-DA faces with a thin TMPTA region having a straight interface with PEG-DA, and two opposite PEG-DA faces having TMPTA corners as shown in Figure 4E. These patchy particles are unique to our technique.

We generated "capped/polymer brush" TMPTA particles by coflowing a mixture of TMPTA-Darocur 1173 with PEG-acrylate solution and exposing to a flash of UV light through a rectangular mask feature, as shown in Figure 4F. The polymeric caps/brushes can act either as a facilitator for directed assembly of particles containing dissimilar chemistry or as a barrier for some specific molecules. The shape concavity can also allow particles with a radius smaller than the radius of the concave curvature to interact with the capped surface, sequestering particles of bigger radius of curvature. Further, two different capping fluids can be used to pattern the two concave curvatures along the plane orthogonal to the plane of projection of light. These particles can be used to selectively adhere to specific sites using one of the caps/patterns and to selectively repel specific molecules using the other cap/pattern. This might be important in avoiding phagocytosis of directed drug delivery systems.[11]

Defining the Phase Space of Particles Generated Using This Technique. A theoretical description of a new class of particles is a daunting task. A plausible route to classifying a new class of particles is the division of the phase space of synthesized particles into anisotropy axis.[44] We divided the phase space of particles generated in this work into 5 anisotropy axis, i.e., nonrectangular feature on mask, concave, convex, chemistry, and patch. The coordinates along the nonrectangular feature on mask axis are 0 or 1, depending on the presence or absence of a rectangular feature on the mask, respectively. Similarly, the coordinates on the concave and convex axis are 0, 1, or 2 depending on the absence or presence on one side or both sides of curvature along the axis orthogonal to the projection of light. The coordinates on the chemistry axis are natural numbers depending on single, double, or multiple chemistries used in the particle. Finally, coordinates on the patchy axis are 0, 1, or 2 depending on the absence or presence of patch on one or both sides of the particle on the axis orthogonal to the plane of projection of light. Capped particles are a special variant of patchy particles with the presence of a layer instead of patch on one or both sides of the polymeric particle. For illustrative purposes, the particle in Figure 1C would have a coordinate of (0,1,0,1,0), i.e., rectangular feature on mask, concave curvature created in the plane orthogonal to the projection of light on one side, convex curvature in the plane orthogonal

to the projection of light on no sides, single chemistry and patchiness on no sides. Similarly, the particles in parts A, E, and H of Figure 2 would have coordinates of (1,1,0,1,0), (1,2,0,1,0), and (1,0,2,1,0), respectively. Some particles in Figure 4, for instance parts A, C, E, and F, would have coordinates of (1,1,0,2,0), (1,1,1,2,0), (0,0,0,2,1), and (0,1,0,2,1), respectively. Having thus divided the phase space of the particles generated by this technique, we can say that particles having 1 as the first coordinate, i.e., particles generated by nonrectangular mask feature, and anything else on the other 4 coordinates are novel and unique to this technique. Furthermore, not all particles having the first coordinate 0 are synthesizable by traditional photolithography or SFL. The presence of patchiness, i.e., 1 or 2 in the fifth coordinate, gives rise to a class of particles which are novel and unique to this technique.

Conclusions

In conclusion, we have demonstrated a facile process for the synthesis of polymeric particles of different chemistries (both hydrophobic and hydrophilic) with finely tuned curvature along the plane orthogonal to the plane of projection of UV light. The fluid interfacial properties and channel height are used to tune the curvature. The dependence of the curvature on these parameters has been mathematically derived and experimentally verified. We have further demonstrated the chemical programmability of this process by the synthesis of patchy and capped particles. Curvature can be used to tune the assembly of these particles giving rise to macrostructures suitable for applications in biology, for instance, for the generation of scaffolds of desired curvature for directing cell internal organization[9] and for improving osteoblast performance to aid tissue formation in bones.[10] Furthermore, the tuned assembly of these particles can be exploited for novel material synthesis for applications in a variety of other fields like photonics, liquid crystals, and optics. Particles with curvature can be used to model the wealth of microscale shapes in nature, be it bacteria, platelets, or erythrocytes. They can also be used in new applications in advanced materials, which take advantage of their unique scattering properties as well as precise control over shape and size.

Acknowledgment. This material is based on work supported by the Singapore-MIT Alliance (SMA-2, CPE Program). The authors thank A. Balducci and D. C. Pregibon for useful discussions.

Supporting Information Available: Experimentally obtained values for the surface tension parameters used for obtaining curvatures; comparison between estimated and experimentally obtained curvatures. This material is available free of charge via the Internet at http://pubs.acs.org.